Pharmaceutical nanotechnology

A cell-free nanofiber composite scaffold regenerated osteochondral defects in miniature pigs

Eva Filová [a,b,*], Michala Rampichová [a,c], Andrej Litvinec [a,d], Milan Držík [e], Andrea Míčková [a,c], Matej Buzgo [a,c], Eva Košťáková [f], Lenka Martinová [f], Dušan Usvald [g], Eva Prosecká [a,c], Jiří Uhlík [h], Jan Motlík [g], Luděk Vajner [h], Evžen Amler [a,c,i]

[a] Institute of Experimental Medicine of the ASCR, Vídenská 1083, 142 20 Prague, Czech Republic
[b] Faculty of Biomedical Engineering, Czech Technical University in Prague, nám. Sítná 3105, 272 01 Kladno, Czech Republic
[c] Department of Biophysics, 2nd Faculty of Medicine, Charles University in Prague, V Úvalu 84, 150 06 Prague, Czech Republic
[d] Institute of Physiology of the ASCR, Vídenská 1083, 142 20 Prague, Czech Republic
[e] Institute of Construction and Architecture, Slovak Academy of Sciences, Dúbravská cesta 9, 845 03 Bratislava 45, Slovak Republic
[f] Textile Faculty, Technical University of Liberec, Studentská 2, 461 17 Liberec, Czech Republic
[g] Institute of Animal Physiology and Genetics of the ASCR, Rumburská 89, 277 21 Liběchov, Czech Republic
[h] Department of Histology and Embryology, 2nd Faculty of Medicine, Charles University in Prague, V Úvalu 84, 150 06 Prague, Czech Republic
[i] Student Science, Horní Podluží 237, 407 57 Horní Podluží, Czech Republic

ARTICLE INFO

ABSTRACT

The aim of the study was to evaluate the effect of a cell-free hyaluronate/type I collagen/fibrin composite scaffold containing polyvinyl alcohol (PVA) nanofibers enriched with liposomes, basic fibroblast growth factor (bFGF) and insulin on the regeneration of osteochondral defects.

A novel drug delivery system was developed on the basis of the intake effect of liposomes encapsulated in PVA nanofibers. Time-controlled release of insulin and bFGF improved MSC viability in vitro. Nanofibers functionalized with liposomes also improved the mechanical characteristics of the composite gel scaffold.

In addition, time-controlled release of insulin and bFGF stimulated MSC recruitment from bone marrow in vivo. Cell-free composite scaffolds containing PVA nanofibers enriched with liposomes, bFGF, and insulin were implanted into seven osteochondral defects of miniature pigs. Control defects were left untreated. After 12 weeks, the composite scaffold had enhanced osteochondral regeneration towards hyaline cartilage and/or fibrocartilage compared with untreated defects that were filled predominantly with fibrous tissue. The cell-free composite scaffold containing PVA nanofibers, liposomes and growth factors enhanced migration of the cells into the defect, and their differentiation into chondrocytes; the scaffold was able to enhance the regeneration of osteochondral defects in minipigs.

© 2013 Elsevier B.V. All rights reserved.

1. Introduction

Cartilage is an avascular tissue with a limited capacity for repair. Standard surgical techniques, such as debridement, penetration of subchondral bone, osteotomy, joint distraction, transplantation of autographs from a non-weight-bearing zone into a defect, and soft tissue grafts, have the potential to stimulate the formation of a new articular surface, and may decrease symptoms and improve joint function. However, they are not able to restore the articular cartilage (Buckwalter and Lohmander, 1994; Buckwalter and Mankin, 1998; Vaquero and Forriol, 2012).

The novel strategy of regeneration of chondral or osteochondral defects so-called matrix-associated involves autologous chondrocyte implantation (MACI) is based on autologous chondrocyte-seeded biomaterials (Trattnig et al., 2005). The matrices already in use in clinical practice include biopolymers, e.g. collagen I/III membrane (Cherubino et al., 2003; Marlovits et al., 2005), hyaluronan derivatives (Trattnig et al., 2005), fibrin (Visna et al., 2004), fibrin/hyaluronate scaffold (BioCart™ II) (Eshed et al., 2012).

Recently, pluripotent mesenchymal stem cells from bone marrow, adipose tissue, or umbilical cord blood were found to differentiate into cartilage, bone or other tissues, depending on growth factors, chemical composition, and the physical and biomechanical properties of the matrices as well as different biomechanical loading of the material (Pittenger et al., 1999; Park et al., 2011a; Jelen et al., 2008). MSC-based therapy has already been used in clinical practice (Haleem et al., 2010). However, bone marrow harvesting is an invasive method that may be demanding for patients.

* Corresponding author at: Institute of Experimental Medicine of the ASCR, Vídeňská 1083, 14220 Prague, Czech Republic. Tel.: +420 296442387; fax: +420 296442387.
E-mail address: evafil@biomed.cas.cz (E. Filová).

In addition, the isolated cells require culture under special conditions, and further implantation. A promising new approach using biomimetic scaffolds guiding cell recruitment from a body niche, e.g. bone marrow, and their subsequent migration into functionalized scaffold has therefore been studied (Sun et al., 2012). This system has great potential in clinical practice, but the optimal parameters need to be found.

Nanofibers have a large specific surface and they can be functionalized with drugs, antibiotics, with bioactive peptides or proteins, RNA, and DNA. (Jannesari et al., 2011; Luong-Van et al., 2006). Sahoo et al. (2010a) reported faster bFGF release from blended nanofibers of poly(lactide-co-glycolide) (PLGA) than from coaxial nanofibers; however, both groups increased the proliferation of MSCs. In another study, a blended PLGA scaffold containing bFGF induced tendon/ligament-like fibroblastic differentiation, including synthesis of type I collagen and tenascin-C (Sahoo et al., 2010b). In our laboratory, we have recently developed systems of nanofibers or microfibers functionalized on the surface (Jakubova et al., 2011; Rampichová et al., 2012), in the core of nanofibers, or in blended nanofibers (Mickova et al., 2012; Buzgo et al., in press) in order to prepare a drug delivery system.

Fibrin gel alone or in composite scaffolds has already been used for repairing cartilage (van Susante et al., 1999; Hunziker, 2001; Eshed et al., 2012; Haleem et al., 2010), bone (Kang et al., 2011), meniscus (Longo et al., 2012), usually with growth factors. Fibrin serves as a drug delivery system where the rate of release is mediated by the interactions between fibrin and chemical, and may be modified by the composition of fibrinogen or thrombin (Spicer and Mikos, 2010).

Hyaluronic acid plays an important role in many physiological and pathological processes, e.g. cell recognition, cell migration, proliferation, cell differentiation, and inflammation. Most of these responses are mediated through the HA-CD 44 interaction (Maniwa et al., 2001; Laurent and Fraser, 1992). A matrix from hyaluronate benzylic esters (HYAFF) was reported to enhance regeneration of osteochondral defects either when seeded with MSCs or when the scaffolds are unseeded (Radice et al., 2000). Biodegradable polymers, such as hyaluronic acid, collagen and fibrin have been already used as scaffolds for drug delivery of growth factors (Holland and Mikos, 2003). Moreover, their three-dimensional structure provides cells with a suitable environment for adhesion, growth and differentiation that is influenced not only by chemical stimuli but also by biomechanical properties. They can also be combined with nano/microparticles, nano/microfibers, or liposomes, which can modify their structure or their biomechanical properties, or can serve for drug delivery.

PVA is a non-toxic, biocompatible material that has been used in medical practice, e.g. as a wound healing material, as an artificial lens, as a material for uterine artery embolization, for dry eye treatment, etc. (McCarron et al., 2011; Walker et al., 2007; Firouznia et al., 2008; Brodwall et al., 1997). The hydrophilic character of PVA means that it swells in water and is water soluble. Longer stability of the material should be achieved by chemical crosslinking (Alipour et al., 2009; Jiang et al., 2009), or by physical methods (Senna et al., 2010; Litvinchuk et al., 2009). As PVA can be successfully electrospun, it is a suitable material for external application, e.g. for wound dressing (Liu et al., 2010), and may be used as a drug delivery system.

Applying these advanced nanofiber scaffolds with a drug delivery system would undoubtedly be advantageous for tissue cartilage regeneration. However, no system of this type has yet been developed. In this study, we prepare nanofibers of a PVA/liposomes blend that are enriched with growth factors bFGF and insulin, and we test the release profile of the growth factors, and their effect on chondrocyte viability in vitro. Then the nanofibers are embedded in a fibrin/type I collagen/fibrin composite hydrogel, and we study their ability to enhance osteochondral regeneration in miniature pigs.

2. Materials and methods

2.1. Housing/animal care

For this study, five male and three female 7-month-old miniature pigs (29 ± 10.5 kg) were used. Animal care was in compliance with the Act of the Czech National Convention for the protection of vertebrate animals used for experimental and other scientific purposes, Collection of laws No. 246/1992, including amendments on the Protection of Animals against Cruelty, and Public Notice of the Ministry of Agriculture of the Czech Republic, and Collection of laws No. 207/2004, on Keeping and Exploitation of Experimental Animals.

2.2. Preparation and characterization of nanofiber scaffolds

50 mL of 12.8% (w/w) polyvinyl alcohol (PVA) solution (Sloviol®, CHZ, Nováky, Slovak Republic) containing 0.38% (w/w) glyoxal (40% (w/w) solution of glyoxal in water) and 0.51% (w/w) H_3PO_4 (85% (w/w) phosphoric acid in water) was prepared, and mixed with 3 mL of liposomes.

Multilamellar liposomes were prepared from 6% phospholipids (Asolectin, from soyabean, Sigma–Aldrich) by dry film method. Briefly, 25 mg of soybean phospholipids were dissolved in chloroform (1 mL) and subsequently evaporated under a flow of N_2 at 4 °C to form a thin lipid film. The dried lipid films were then resuspended in 3 mL of 100 mM phosphate buffer saline (PBS) at pH 7.3 for the preparation of empty liposomes. We used liposome mixture instead of pure phospholipids to facilitate the preparation of emulsion of phospholids in PVA solution for electrospinning. The emulsion was intensively stirred for 30 min. Electrospinning was carried out on a Nanospider™ device as described previously in detail (Lukáš et al., 2008). A high-voltage source generated voltages of up to 56 kV, and the polymer solutions were connected with the high-voltage electrode. The electrospun nanofibers were deposited on a grounded wire collector electrode. The distance between the top of the rotating drum and the collecting plate was 12 cm. All electrospinning processes were performed at room temperature (RT; ~22 °C) and a humidity of ~50%.

The nanofibers that were formed were crosslinked at 135 °C for 10 min and then dried in a desiccator. PVA nanofibers without liposomes were prepared as a control.

The surface morphology was studied using a Vega scanning electron microscope (Tescan, Czech Republic). The tested materials are not good conductive materials; a gold coating was therefore applied on the surface to increase the surface conductivity of the electrospun materials. From five SEM photomicrographs of both PVA + LIP and PVA nanofibers, the pore diameter and the pore size of the nanofibers were measured, and the porosities were calculated using LUCIA G Image Analysis, version 4.82 (Laboratory Imaging Ltd., Czech Republic). Nanofibers with the similar surface density were used.

2.3. Release of the growth factors from the nanofibers

PVA scaffold with liposomes was cut into round patches, with the area of 5 cm^2, weighing 11.3 ± 1.6 mg (mean and SD), and then four samples were incubated in PBS solution containing 200 µg/mL insulin (Actrapid inj. 100 IU/mL) and 200 ng/mL basic Fibroblast growth factor (bFGF, human recombinant, Roche Applied Science) at room temperature (RT) for 30 min (PVA + LIP). Four PVA nanofiber scaffolds without liposomes but with the same amount of growth factors were prepared as controls (PVA group). The scaffolds were

washed twice with PBS to avoid the excess of growth factors adsorbed on the surface, and then incubated in 1 mL PBS for 18 days at 37 °C; the PBS was completely changed and stored at −20 °C until the measurement had been performed. The time interval was determined keeping in mind a balance between the release of a detectable amount of growth factors and maintenance of the sink condition. The amount of insulin and bFGF released into the PBS was measured using Enzyme-Linked ImmunoSorbent Assay (ELISA), (human insulin ELISA E0448h, Uscn Life Science Inc. and bFGF DuoSet ELISA, DY233, R&D Systems, respectively) according to the manufacturer's instructions, except that the bFGF–antibody complex was detected by chemiluminescent reactions initiated by the addition of 100 μL of substrate solution SuperSignal ELISA Pico (Pierce) to each well. The luminescence was measured at 420 nm for 30 s using a Perkin-Elmer LS 50B luminescence spectrometer, and the concentration of bFGF was determined using a six-point calibration curve. Both the absolute release profile and the cumulative release profiles were calculated from four parallel samples for both growth factors. The half-time of release (τ) was determined as the time at which the initial concentration c_0 had decreased to $c = 1 - (c_0 \cdot e^{-1})$. ELISA experiments were done at 22 °C.

2.4. Isolation, and culture of mesenchymal stem cells on nanofibers enriched with growth factors – cell viability evaluation

Bone blood marrow was taken under general anesthesia from the iliac bone of a miniature pig, according to Prosecká et al. (2012). The second passage of mesenchymal stem cells (MSCs) was used for an in vitro study.

PVA nanofibers with liposomes were cut into a circle 6 mm in diameter, and were then incubated with PBS solution containing 200 μg/mL insulin (Actrapid inj. 100 IU/mL) and 200 ng/mL basic Fibroblast growth factor (bFGF, human recombinant, Roche Applied Science) at room temperature (RT) for 30 min. The growth factor-modified nanofibers (PVAGF 1%), and the control PVA scaffold without growth factors (PVA 1% or PVA 10%) were seeded with MSC (100×10^3 cells/cm^2) in a medium containing 1% or 10% (w/v) fetal bovine serum (FBS), respectively, and cultured for 7 days.

The cell viability was analyzed using the MTT test (Jakubova et al., 2011). The optical density of 200 μL solution was measured ($\lambda_{sample} = 570$ nm, $\lambda_{reference} = 690$ nm). The absorbance of the samples incubated without cells was deducted from the cell-seeded samples.

In addition, MSCs adhered to scaffolds 1 day after seeding were stained using mouse monoclonal antibody against β-actin, followed by goat anti-mouse AlexaFluor 488 secondary antibody (A, C, E), and were visualized by confocal microscopy (Zeiss LSM 5 DUO) ($\lambda_{exc} = 488$ nm, $\lambda_{em} = 505$–550 nm). On days 1 and 7, live/dead staining was applied and the cells were visualized for propidium iodide and BCECF signal (Jakubova et al., 2011).

2.5. Biomechanical evaluation

The purpose of biomechanical testing was to determine the dynamic compressive loading diagrams, and also to evaluate the development of material stiffness or Young's modulus under compression deformation. The impact testing procedure was performed using a pendulum-like machine for unconfined compression of cylindrically-shaped samples as we previously described (Varga et al., 2007; Handl et al., 2010) at 24 °C. The circular contact area of the specimens was chosen with diameter $\phi = 5.5$ mm, and the specimens varied in thickness from 2.2 mm to 4.8 mm. The weight strikes a specimen that is positioned perpendicular to the motion of the weight. The process is tracked using a single detector, e.g. a piezoelectric accelerometer. Continual reading of the time traces for displacement, velocity and acceleration within the impact provides

all the information required for determining the continuous loading force and also the compression of the tested specimen.

To characterize the individual samples, five measurements were carried out at each of four different impact energies. Thus, several trials were recorded on each sample to test the statistical dispersion and the reproducibility of the measurements at the same load (impact energy).

Four types of artificial materials were used in the study – fibrin gel with and without PVA nanofibers ($1\times$ NF Fibrin, and Fibrin, respectively), and the composite scaffold of the compound of fibrin, hyaluronic acid and type I collagen, also with and without nanofibers ($1\times$ NF Composite Scaffold, and Composite Scaffold, respectively). The basic materials, in which no nanofibers were included, were evaluated for comparison. A total of three samples were measured for each of the materials.

2.6. Thermogravimetric analysis

Thermogravimetric analysis (TGA) was performed using a Pyris 1 TGA thermogravimetric analyzer (Perkin-Elmer, USA) in a nitrogen atmosphere. Dry nanofibers were heated at a constant heating rate of 5 °C/min in the range of 35–800 °C. The dry nanofiber samples weighed approximately 1–2 mg. The structure of nanofibers did not allow using higher mass of the samples. The hydrogel samples were heated at a constant heating rate of 10 °C/min, from room temperature to 85 °C. Isothermal heating was maintained for the following 40 min at 85 °C; subsequently the temperature was increased to 150 °C at a heating rate of 10 °C/min and maintained for 5 min. The hydrogels weighed approximately, 25 mg the surface was dried with filter paper before the analysis. Three samples for each group were used for the measurements.

2.7. Preparation of the fibrin scaffold containing growth factor-modified nanofibers and implantation of the scaffold in vivo

One day before the operation, the nanofibers were cut into small pieces (1×2 mm); the mesh was incubated in a mixture of 200 ng/mL bFGF and 200 μg/mL insulin at room temperature (RT) for 30 min. Then the scaffold was washed with PBS and mixed with the culture medium – Iscove's modified Dulbecco's Medium (I3390, Sigma–Aldrich) supplemented with 10% fetal bovine serum (FBS), 100 IU penicillin, 100 μg/mL streptomycin, 4 mM L-glutamine, and 40 μg/mL L-ascorbate-2-phosphate sesqui-magnesium salt. The nanofiber mesh (80 mg/mL) was embedded in a fibrin gel, as has been previously reported (Filová et al., 2007, 2008). Briefly, 31.58 μL of type I collagen solution in 0.1 M acetic acid (Collagen type I from calf skin, acid soluble, Sigma) was neutralized with 1 M KOH at about 4 °C; 21 μL sodium hyaluronate (10 mg/mL, 1500 kDa, kindly provided by CPN, CR) and nanofibers in a medium were added into the well. Additionally, 100.8 μL of Tissucol® solution in aprotinine (fibrinogen 70–110 mg/mL, aprotinine 3000 KIU/mL), and 100.8 μL/mL of thrombin solution (4 IU/mL) in CaCl$_2$ (40 μmol/mL, Tissucol® Kit, Baxter) were mixed in with the nanofiber mixture. The gels were formed at 37 °C. Subsequently, a culture medium was added, and the scaffolds were placed in an incubator with a humidified atmosphere, 5% CO$_2$ at 37 °C for 1 day.

The surgery was performed under general anesthesia. Having the operation field been prepared, lateral arthrotomy of the right knee joint with medial luxation of the patella was performed. The fibrin scaffold containing growth factor-enriched nanofibers was implanted into the load-bearing part of the right femoral condyle of eight miniature pigs. A scaffold was introduced into the circular defect 8 mm in diameter. The scaffold was fixed in situ with Tissucol® tissue adhesive. As controls, two circular osteochondral defects were drilled in the left knees of each animal; the defects

Table 1
Software analysis of SEM photomicrographs of the nanofiber scaffold showed the diameter of the submicroscopic fibers in scaffolds with significantly larger fiber diameter and also bigger pore size for polyvinyl alcohol PVA nanofibers than for PVA nanofibers with liposomes (PVA + LIP) (mean ± standard deviation).

Nanofiber scaffold	Fiber diameter (nm)	Pore size (μm^2)	Porosity	Number of measurements
PVA	285 ± 91[*]	0.268 ± 0.28[*]	0.249	670
PVA + LIP	258 ± 79	0.206 ± 0.22	0.256	900

[*] $p \leq 0.001$.

were left untreated. All lesions were sutured in the observed layers: the joint theca, muscles and subcutis using absorbable catgut, the cutis with a non-absorbable material. The sutures in the cutis were removed 12 days after the operation. All the animals received preventive doses of antibiotics (Peni-Kel 300; 8000 I.U./kg b.w.) and analgesics (Vetalgin inj. ad us. vet. – metamizolum; 30 mg/kg b.w.) by intramuscular administration.

All animals were euthanized using a stun gun 12 weeks after implantation of the scaffold. The femoral condyles, including the site where the test item had been administered, were sampled and fixed in 4% phosphate buffered formaldehyde for histological examination.

2.8. Histology

The bones were decalcified with ethylenediaminetetraacetic acid. Histological slides were made by a routine paraffin technique, and stained with haematoxylin and eosin (HE), a combined staining technique using Alcian Blue at pH 2.5 followed by PAS-reaction for mucosubstances, van Gieson stain, orcein, and the Gomori method. In addition, we used immunohistochemical evidence of type II collagen using mouse monoclonal primary antibody against type II collagen, clone II-II6B3 (1:10 dilution), obtained from Developmental Studies Hybridoma Bank, developed under the auspices of the NICHD and maintained by the Department of Biological Sciences, University of Iowa, Iowa City, IA 52242; visualization was performed with rabbit polyclonal secondary anti-mouse horseradish peroxidase-labeled antibody (Sigma A 9004) and a SIGMAFAST™ 3,3′-diaminobenzidine, followed by haematoxylin counterstaining. For the assessment, we used NIS Elements AR 3.0 image analyzer software (Laboratory Imaging, Prague, CR).

2.9. The histological and histochemical scoring system

The repairs to the osteochondral defects in all groups were compared using a scoring system for histological and histochemical results with a maximum of 24 points, modified from Susante et al. (1999). One defect from each knee was analyzed statistically. The blind analysis was performed by two of the authors of this paper.

2.10. Histomorphometry

The measurement of all defects was performed according to Filová et al. (2007), and the evaluation was performed according to Breinan et al. (2001).

2.11. Statistical analysis

Quantitative data was presented as mean ± SD (standard deviation). A statistical analysis was performed using One Way Analysis of Variance (ANOVA) and the Student–Newman Keuls Method. The level of significance was set at 0.05.

3. Results

3.1. PVA nanofibers had a higher fiber diameter and higher pore size than PVA nanofibers with liposomes

Small unilamellar phosphatidylcholine liposomes were prepared, added to PVA solution and this blend was used for nanofiber preparation. Notably, liposomes were assembled from 6% phospholipids (Asolectin) in 100 mM phosphate buffer at pH 7.3, i.e. without any encapsulated bioactive substance. Both pure PVA and a PVA blend with liposomes (PVA + LIP) were successfully electrospun, and nanofibers were formed. Photomicrographs from SEM showed a submicroscopic fiber diameter with a higher pore diameter (285 ± 91 nm, and 258 ± 79 nm, respectively), and also higher pore size (0.268 ± 0.28 μm^2, and 0.206 ± 0.22 μm^2) of PVA nanofibers compared to PVA + LIP, and similar porosity (Table 1). In addition, specific structures were seen on the surface of PVA + LIP (Fig. 1).

3.2. Liposome-enriched nanofibers with encapsulated insulin and bFGF showed controlled release of both growth factors, but resulted in higher absolute release of insulin

Nanofibers either with or without incorporated liposomes were incubated with insulin and bFGF, and the concentration of the released growth factors was determined by sandwich ELISA. The amount of encapsulated insulin was 145.98 μg for PVA + LIP and 73.72 μg for PVA. The amount of encapsulated bFGF was 10.78 ng for PVA + LIP and 11.1 ng for PVA. In the case of bFGF, the cumulative release profile showed controlled release of bFGF from the nanofibers both for PVA with incorporated liposomes (PVA + LIP) and for PVA without incorporated liposomes (PVA); the curves of bFGF for both PVA + LIP and PVA were nearly identical, therefore they look like one curve (Fig. 2). The half-time of release was also similar for both samples ($\tau_{PVA+LIP} = 11.4$ days, $\tau_{PVA} = 11.6$ days). Similar absolute release of bFGF was also observed (10.78 ng for PVA + LIP, and 11.1 ng for PVA).

In the case of insulin, the cumulative release profile showed faster release than for bFGF. However, the cumulative release profiles for samples with and without liposomes were also similar ($\tau_{PVA+LIP} = 5.2$ days, $\tau_{PVA} = 5.7$ days). Interestingly, the absolute release profile of PVA nanofibers with liposomes showed a significantly higher release of insulin (PVA + LIP = 146 μg) than the sample without incorporated liposomes (PVA = 73.7 μg).

3.3. Both in the MTT assay and in confocal microscopy, growth factor-enriched PVA nanofibers with liposomes showed improved cell viability

Throughout the experiment, PVA + LIP 1% GF nanofibers that were cultured in the medium with 1% FBS displayed significantly higher absorbance in MTT than the same nanofibers without growth factors (PVA + LIP 1%), and also significantly higher absorbance in MTT than pure nanofibers cultured in the medium
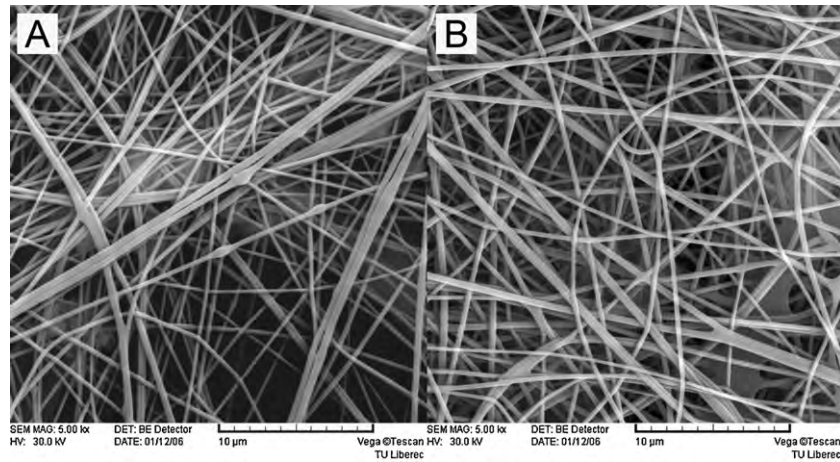
Fig. 1. Scanning electron microscopy of nanofibers.
Scanning electron microscopy of polyvinyl alcohol nanofibers with incorporated liposomes (PVA + LIP) (A) and pure PVA nanofibers (PVA) (B) showed submicroscopic fibers of large diameter and large pore size in the PVA scaffold. The round patches may be survived intact incorporated liposomes, or bulges of polymer.
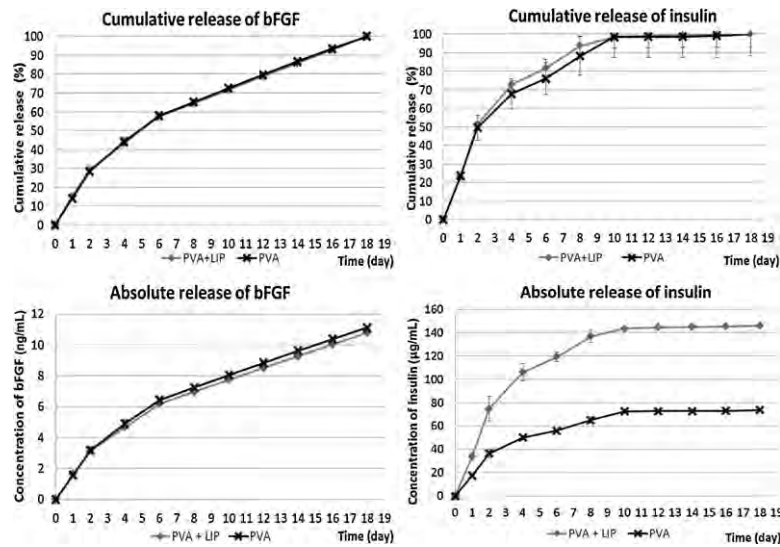
Fig. 2. Release of growth factors from nanofibers.
The cumulative release of both bFGF and insulin showed no significant changes between pure PVA nanofibers (PVA) and PVA with incorporated liposomes (PVA + LIP); however, the insulin release rate was faster than the release rate of bFGF. The absolute release of bFGF showed no changes between PVA and PVA + LIP. The absolute release of insulin from PVA + LIP was significantly higher than the release of insulin from PVA.

with 10% FBS (PVA 10%). Moreover, on day 1, absorbance of PVA 10% was significantly higher than that of PVA + LIP 1% (Fig. 3).

Confocal microscopy photomicrographs showed that a small number of cells were adhered to all scaffolds. However, on day 1 there was a higher number of cells, and, on day 7, better cell viability was seen on the PVA + LIP 1% GF scaffold than on PVA 10% and PVA + LIP 1% (Fig. 4).

3.4. Nanofiber-enriched composite gel produced slightly improved viscoelastic properties

Fig. 5 presents illustrative examples of loading diagrams of selected samples of various materials. For each sample, the impact energy of the loading and the initial thickness of the samples are presented. The hysteresis curves characterize the internal damping of the material.

In addition to the curves of the compressive forces and the corresponding compression displacements, we also evaluated the developments of tangent Young's modulus vs. compression strains (see Fig. 6). The tangent Young's modulus must be expressed as the
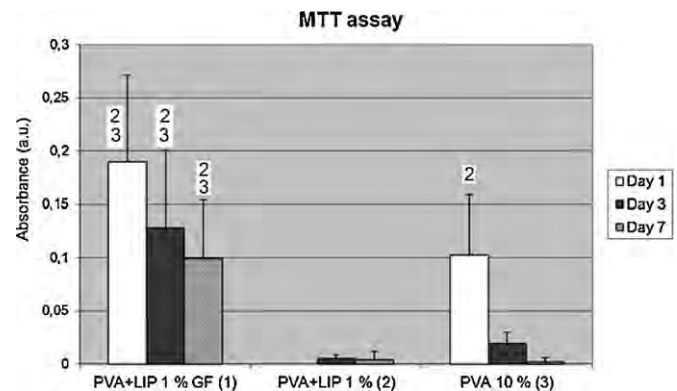
Fig. 3. MTT assay.
MTT assay showed significantly higher viability of chondrocytes seeded on polyvinyl alcohol scaffolds modified with growth factor-enriched liposomes (PVA + LIP 1% GF) than on other scaffolds, e.g. the control scaffold without GF (PVA + LIP 1%), both were cultured with 1% fetal bovine serum (FBS), and on the control pure PVA nanofibers cultured in the presence of 10% FBS (PVA 10%).
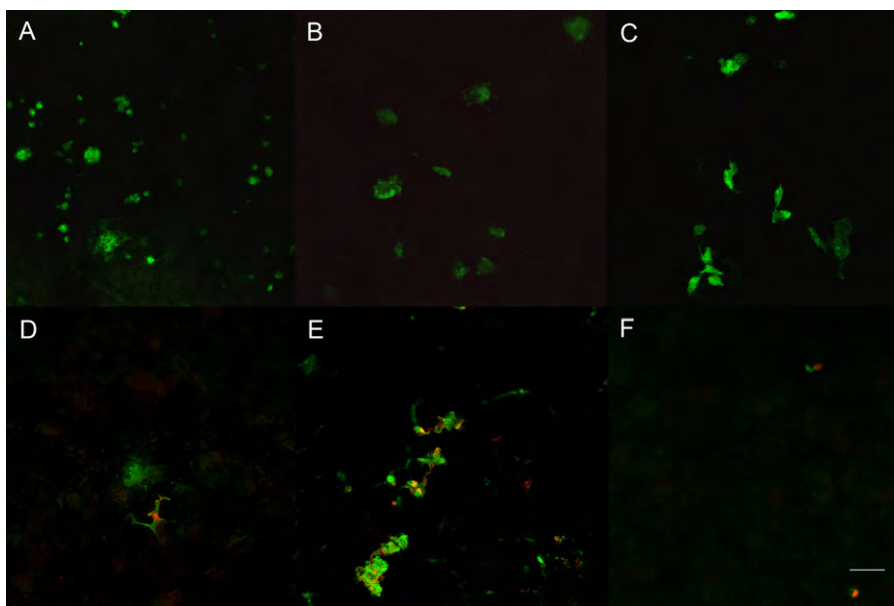
Fig. 4. Confocal microscopy of MSC-seeded nanofibers.
Cells adhered on scaffolds 1 day after seeding were stained using mouse monoclonal antibody against β-actin, followed by goat anti-mouse AlexaFluor 488 secondary antibody (A, B, C) and visualized by confocal microscopy. On day 1, higher densities of MSCs were observed on the PVA scaffold modified with growth factor-enriched liposomes (PVA + LIP 1% GF) (B) and on the control pure PVA (PVA 10%) (C) cultured in either 1% or 10% of foetal bovine serum (FBS), respectively compared to PVA with liposomes without growth factors (PVA + LIP 1%) (A) that was cultured in a medium with 1% FBS. On day 7, live/dead staining (D, E, F) showed viable MSCs on the PVA + LIP 1% GF (E), while only a few solitary cells were observed on the PVA + LIP 1% scaffold (D) and on the PVA 10% scaffold (F) (Obj. 20, magnification ×2, bar = 50 μm).

value defined as the slope of the tangent line to the compressive force vs. displacement or alternatively strain diagram. The error variances were estimated taking into account possible experimental errors in determining the initial thickness of the sample, as well as the impact velocity and the position of the mechanical contact at the beginning of the loading. The initial mechanical contact of the pendulum weight and the tested sample is strongly affected by any irregularity of the contact surface, so the reading begins at the defined preload force (0.3 N). Precise determination of the

beginning of sample loading (see Fig. 5) was the main factor in the uncertainty.

As the impact energy has to be damped, the stiffness values, and consequently the tangent modulus of elasticity values, must show a significant increase in the higher range of the graphs, particularly for higher impact energies. After statistical treatment, a comparison of the composite scaffold and the fibrin gel showed that the composite scaffold and the fibrin gel with added nanofibers seem to be slightly stiffer, and with a higher Young's modulus, than the fibrin gel or the composite scaffold without nanofibers. Although the stiffness of the fibrin gel with a small concentration
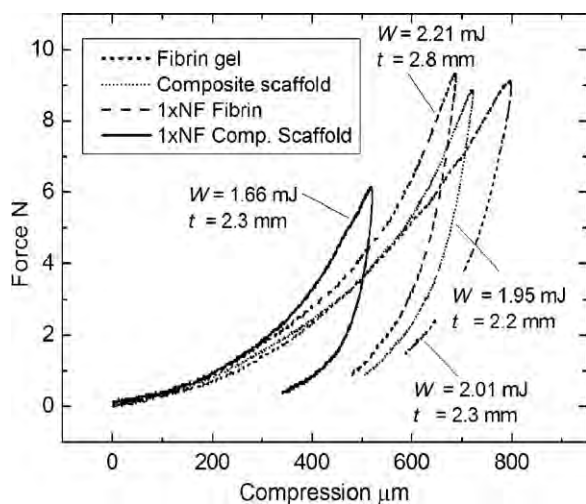
Fig. 5. Dynamic loading diagram of artificial cartilage materials.
Typical dynamic loading diagrams of artificial cartilage material substitutes, such as fibrin, composite scaffold consisting of hyaluronate, type I collagen, fibrin (composite scaffold), and both scaffolds containing the same amount of nanofiber pieces as was used in a pig study (e.g. 1× NF fibrin or 1 × NF composite scaffold), at the defined impact energy W for different samples thickness t. The hysteresis curves characterize the internal damping of the material. The fibrin gel based materials show less stiffness.
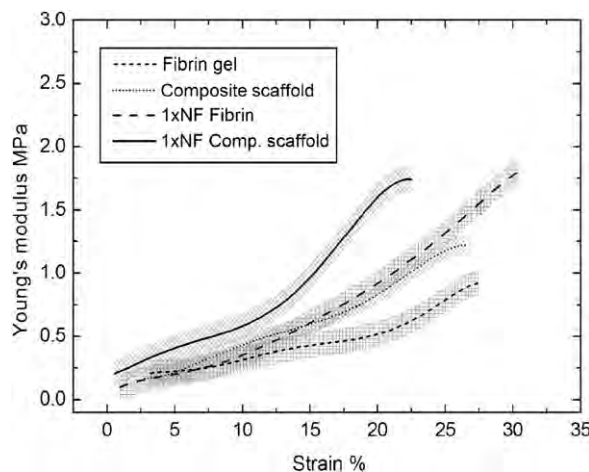
Fig. 6. Young's modulus course in artificial cartilage materials.
The courses of tangent Young's modulus development vs. strain for articular cartilage substitutes fibrin gel, composite hyaluronate/type I collagen/fibrin gel (composite scaffold) and the same scaffolds containing the same amount of nanofibers that were used in a pig study (1× NF Fibrin, 1× composite scaffolds) as a substitute for articular cartilage. Typical curves are drawn which statistically represent nearly mean values obtained as the average of several samples of the same material. The estimated error variance band is plotted for each type of material.

Table 2
Thermogravimetric measurement of the water content (w/w) of four different hydrogel samples: fibrin gel, composite type I collagen/hyaluronate sodium/fibrin gel (Composite gel), composite gel containing nanofibers from polyvinyl alcohol (PVA composite gel), and composite gel containing PVA nanofibers with liposomes (PVA + LIP composite gel). The measurements showed a significantly higher water content in the PVA composite gel than in the other scaffolds (mean ± standard deviation).

Hydrogels	Water content (%)
Fibrin gel	87.4 ± 0.2
Composite gel	87.8 ± 0.44
PVA composite gel	89.7 ± 0.2[*]
PVA + LIP composite gel	87.5 ± 0.42

[*] $p \leq 0.001$.

of nanofibers (1× NF Fibrin) is not far from the stiffness of the pure fibrin gel, and the same is true also for the nanofiber composite scaffold compared to the scaffold without nanofibers, there is a detectable enhancement in stiffness. Thus nanofibers can play a significant role in the mechanical properties of the material. This suggests that the desirable biomechanical properties can probably be improved considerably by adding more nanofibers into the fibrin.

3.5. Liposome-enriched nanofibers decreased the water content both in PVA nanofiber-enriched fibrin and in a composite scaffold

Dry PVA and PVA + LIP nanofibers contained a similar amount of free adsorbed water on the scaffold surface (4.6 ± 0.9% in PVA, and 4.8 ± 0.8% in PVA + LIP). However, at temperatures higher than 100 °C, the maximum weight loss was observed at 150 °C. The maximum weight loss that corresponds to the amount of immobilized water was significantly higher in PVA than in PVA + LIP (PVA 8.6 ± 0.1%, PVA + LIP 4.0 ± 0.1%).

All hydrogels showed considerable weight loss even at a low temperature. However, a significantly higher water content was measured in the PVA composite gel (e.g. containing PVA nanofibers without liposomes) than in the other hydrogels – fibrin, hyaluronate sodium/type I collagen/fibrin composite scaffold (Composite scaffold), and PVA + LIP composite scaffold (e.g. containing PVA nanofibers with liposomes) (Table 2).

3.6. Histology

3.6.1. Scaffold group
The scaffolds were implanted into osteochondral defects 8 mm in width and 2.7 ± 0.9 mm in depth in a load-bearing part of the right lateral femoral condyle. A thin acellular layer (0.056 ± 0.005 mm in width) was found on the borders of the defects. The regeneration of osteochondral defects was characterized by the regular formation of isogenic rows of chondrocytes near the bases of the defect with a mean length of 0.58 ± 0.23 mm, and by differentiation towards cartilage. In the central or upper part of the defects, chondroblasts were present (Fig. 7A and C).

In the upper half of the defect, fibrocartilage was found with occasional dense irregular connective tissue on the surface of the defect. Neither an inflammatory reaction nor osteophyte formation was observed in the regenerated cartilage.

At first, the differentiation was accompanied by vascularization, but no blood vessels were found in the deeper part of the defects. In the upper parts of the defects, fine granular or fibrous intercellular material and also some small blood vessels were observed.

The acellular zone and the cartilage at the borders and in the middle part of the defects were predominantly alcian blue-positive in all repaired defects. In all animals, the basal zone was predominantly alcian blue-positive; moreover, in two animals, weak

PAS-positive staining was observed in the basis. The fine granular material was PAS-positive, while the fibrous surface zone showed weak PAS-positive staining (Fig. 7C).

The zone at the border of the extracellular matrix between the normal adjacent cartilage and the newly formed fibrocartilage was found to be type II collagen positive (Fig. 7G). However, the adjacent cartilage and the new fibrocartilage were found to be negative. Positive staining of type II collagen was also found in the dense collagenous layer on the surface of the defect (Fig. 7E) as well as in the wall of the vessels and/or near the vessels.

3.6.2. Control group
A total of 16 defects were introduced in the medial and lateral condyles of eight minipigs. The depth of the osteochondral defects measured in the photomicrographs was 3.6 ± 1.2 mm. An acellular zone 0.07 ± 0.03 mm in width was found on the borders of the defects. In nine defects, the regeneration was characterized by differentiation to fibrocartilage or irregular dense connective tissue with isogenic rows of chondrocytes of 0.1 ± 0.1 mm in mean length situated at the borders of the defect (Fig. 7B and D); the regeneration was rarely accompanied by bone trabecules, or even by osteophyte formation with an inflammatory reaction in the basis of the defect. The differentiation was predominantly accompanied by vascularization; however, some vessels revealed signs of the fibrinoid necrosis. Five defects were only partially covered by a thin layer of connective tissue with isogenic rows of chondrocytes 0.02 ± 0.03 mm in length.

Large deposits of alcian blue-positive material were found around cells and fibers in the upper part of the defects; only faint PAS-positive staining was observed in the surface layer. The fine granular material was also PAS-positive, but only faint PAS-positivity was observed in the basal layer in the axis of the defects (Fig. 7D).

Type II collagen staining was positive in the transition zone between the newly formed tissue and the adjacent cartilage; the chondrocytes near the border of the adjacent cartilage were also positive. Moreover, in the vascularized defects, the extracellular matrix of the fibrous tissue around the vessels was positive (Fig. 7F and H).

3.7. Histological and histochemical score

The scaffold group showed a significantly higher histological and histochemical score than the control group (score for the scaffold group: 18 ± 2, score for the control group: 12 ± 3, mean and standard deviation) (Table 3). Improved properties of the newly formed tissue were observed in the nature of the predominant tissue (except for Bonding to the Adjacent Cartilage) and also in the properties of the adjacent cartilage.

3.8. Histomorphometry

In the scaffold group, the predominant tissue of the defect was fibrocartilage (66.8 ± 23.6%), while in the controls the dense irregular connective tissue (63.7 ± 24%) was predominantly found in the defects. In the scaffold group, a significantly higher amount of fibrocartilage and a significantly lower amount of dense irregular connective tissue were measured than in the controls (Table 4).

4. Discussion

4.1. A novel drug delivery system based on the intake effect of liposomes encapsulated in PVA nanofibers

Phospholipid liposomes are known as a well-described drug delivery system (Levchenko et al., 2012; Ulrich, 2002). Clearly,
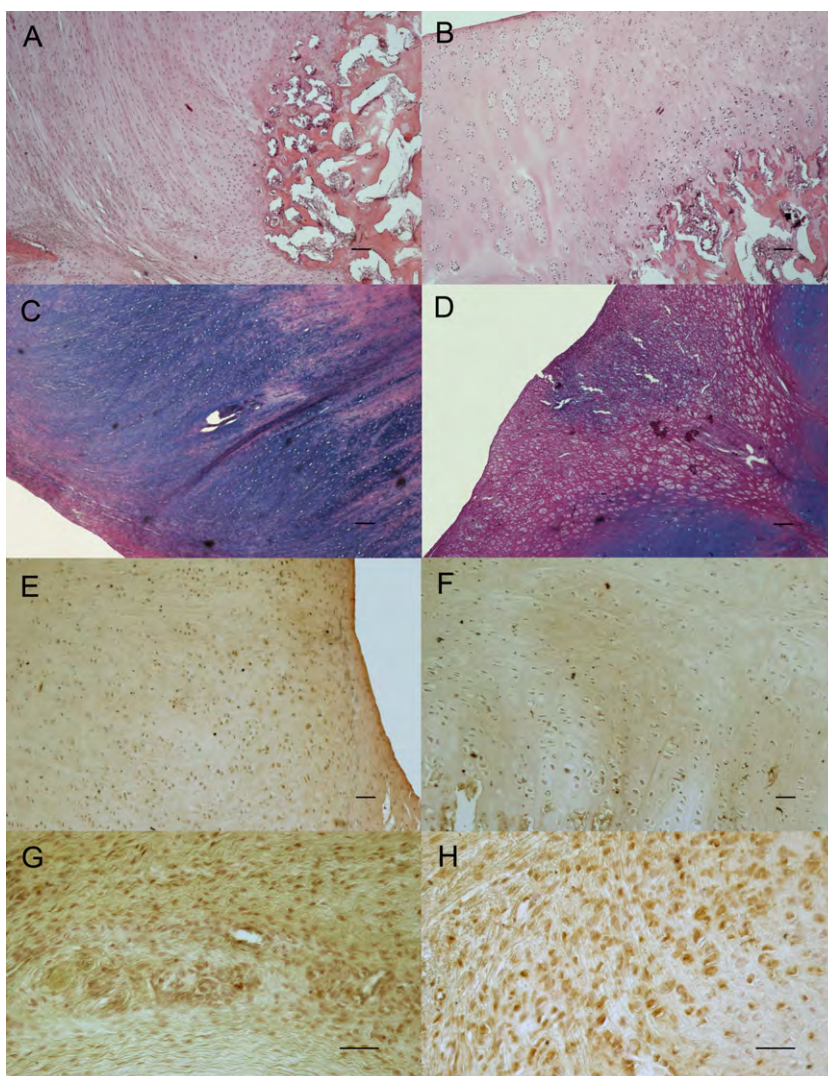
Fig. 7. Histological evaluation.
Histology of the osteochondral defect of the scaffold group treated with hyaluronate/type I collagen/fibrin composite gel with polyvinyl alcohol nanofibers enriched with liposomes, bFGF, and insulin (A, C, E, G) and untreated controls (B, D, F, H) 12 weeks after implantation using HE staining (A, B), Alcian blue staining and PAS-reaction at pH 2.5 (C, D), and immunohistochemical staining using monoclonal antibody against type II collagen (E–H). The repaired tissue in the scaffold group contained differentiated chondrocytes, which were randomly organized within mostly fibrocartilage or hyaline cartilage containing high amounts of GAGs (C) and type II collagen (E, G). Type II collagen shows strong diffuse positivity in the upper part of the repaired tissue (E); strong positivity of the tissue can be seen at the edge of the proliferating cartilage growing into the bone (F–H). Magnification: ×100 (A–D), ×200 (E, F), ×400 (G, F), bar = 100 μm (A–D) and 50 μm (E–H).(For interpretation of the references to color in this figure legend, the reader is referred to the web version of the article.)

liposomes with an appropriate membrane lateral pressure have a prospective to accommodate both polar and hydrophobic compounds, due to the polar heads and hydrophobic fatty acid chains of phospholipids (Konopasek et al., 1995). Moreover, the aqueous liposomal core is an ideal microenvironment for accumulation and traffic of polar compounds. We have shown that a system of this kind can retain and accumulate compounds that can bind to or penetrate through a lipid bilayer. Taking advantage of these special properties, we have developed a drug delivery system based on a soaking effect of PVA nanofibers enriched with liposomes.

The electrospinning process resulted in the formation of sub-micrometer fibers. The round patches present in the liposome nanofiber picture (Fig. 1) may be survived intact incorporated liposomes, or bulges of polymer formed due to Raleigh instability. Fibers with embedded liposomes were smaller in mean size, which is preferable for cell adhesion. However, the process also resulted in small pore size, which is associated with lower penetration of cells to the scaffold (Pham et al., 2006). We have recently reported that electrospinning resulted in the survival of at least 40%

of intact liposomes in a PVA blend and the incorporation ratio of phospholipids into nanofibers prepared by blend electrospinning was $57.1 \pm 5.8\%$ (w/w) (Mickova et al., 2012). The high crosslinking temperature (135 °C) can degrade liposomes; however, our aim was to modify the character of PVA nanofibers, which are highly hydrophilic. The process enriched the fibrous mass with phosphatidylcholine membranes, changed the hydrophilic character of nanofibers into more hydrophobic, and moreover, decreased the water content both in PVA nanofiber-enriched fibrin and in a composite scaffold. This type of system has different physical and chemical properties, which are associated with altered drug delivery potential.

4.2. Time-controlled release of insulin and bFGF improved MSC viability in vitro

Non-modified PVA nanofibrous scaffolds are highly hydrophilic (Liu et al., 2010). Clearly, the hydrophilic character of the PVA scaffold and its high water uptake contribute to successful wound

Table 3
Histological and histochemical scoring system, modified from van Susante et al. (1999); growth factor-modified scaffolds implanted in osteochondral defects (Scaffolds) achieved a significantly higher score than untreated defects (Controls).

		Scaffolds	Controls
Nature of predominant tissue			
Cellular morphology (I)			
Hyaline articular cartilage	(4)	0	0
Incompletely differentiated	(2)	6	4
Dense connective tissue and bone	(0)	1	4
Alcian blue staining of the matrix (II)			
Normal or near normal	(3)	3	0
Moderate	(2)	4	4
Slight	(1)	0	4
None	(0)	0	0
Structural characteristics			
Surface regularity (III)			
Smooth and intact	(3)	5	0
Superficial horizontal lamination	(2)	2	5
Fissures, 25–100% of the thickness	(1)	0	3
Severe disruption or fibrillation	(0)	0	0
Structural integrity (IV)			
Normal	(2)	2	0
Slight disruption, including cysts	(1)	5	5
Severe disintegration	(0)	0	3
Thickness (V)			
100% of normal adjacent cartilage	(2)	7	3
50–100% of normal cartilage	(1)	0	5
0–50% of normal cartilage	(0)	0	0
Bonding to the adjacent tissue (VI)			
Bonded at both sides and subchondral bone	(2)	2	7
Bonded partially	(1)	5	1
Not bonded	(0)	0	0
Freedom from cellular changes of degeneration			
Hypocellularity (VII)			
None	(3)	3	0
Slight	(2)	4	4
Moderate	(1)	0	3
Severe	(0)	0	1
Chondrocyte clustering (VIII)			
None	(2)	5	3
<25% of cells	(1)	2	3
25–100% of cells	(0)	0	2
Freedom from degenerative changes in adjacent cartilage (IX)			
Normal cellularity, no clusters, normal staining	(3)	1	0
Normal cellularity, mild clusters, moderate staining	(2)	5	2
Mild or moderate hypocellularity, slight staining	(1)	1	6
Severe hypocellularity, poor or no staining	(0)	0	0

healing (Liu et al., 2010). Semi-solid or gel PVA was successfully tested for sustained release of local anesthetic lidocain (McCarron et al., 2011), or gentamycin (Hwang et al., 2010). We tested a novel composite system of PVA nanofibers functionalized with phosphatidylcholine liposomes in vitro for drug uptake and release.

Table 4
A histomorphometric evaluation of defects showed a significantly higher amount of fibrocartilage and a significantly lower amount of dense irregular connective tissue in osteochondral defects with growth factor-modified composite type I collagen/hyaluronate sodium/fibrin gel with liposomes (Scaffolds) than for untreated defects (Controls).

	Hyaline cartilage (%)	Fibrocartilage (%)	Dense connective tissue (%)
Scaffolds	7.8 ± 6.7	66.8 ± 23.6[*]	25.3 ± 26.7
Controls	9.3 ± 12.6	28.5 ± 27	63.7 ± 24[*]

[*] $p \leq 0.05$.

Insulin comprises polar areas and non-polar areas (Blundell et al., 1971), and was reported to interact with phosphatidyl choline bilayers (Wiessner and Hwang, 1982). In addition, insulin distribution was reported to be higher among unsaturated hydrocarbon chains of phospholipids than among saturated chains (Schwinke et al., 1983).

Insulin was therefore selected as a model drug for probing the availability of liposomal membranes embedded in nanofibers for the interaction with proteins. By contrast, bFGF was selected as a growth factor that was not reported to interact with phosphatidyl choline membranes. Our data showed that the presence of liposomes in the blend did not affect the cumulative release either of bFGF or of insulin. However, the absolute amount of adsorbed insulin was significantly higher for liposome-enriched nanofibers than for pure nanofibers. No such difference was observed in the case of bFGF. This kind of difference could be very useful in tissue engineering, and in a general drug delivery system. The system enabled longer release than the liposomal system proposed by Park et al., who reported initial burst release of 34–46% insulin in 30 min, and the slower release of 48–73% insulin from PEGylated liposomes, and the release of 55–100% insulin from plain liposomes over 72 h (Park et al., 2011b). Additionally, the growth factors were immobilized on the scaffold and were thus prevented from washing out from the injury site. In fact, insulin- and bFGF-enriched PVA nanofiber with embedded liposomes significantly increased the MSC viability in our in vitro experiment (Figs. 3 and 4).

4.3. Nanofibers functionalized with liposomes improved the mechanical characteristics of a composite gel scaffold

In order to test the performance of the system in vivo, we developed a composite gel functionalized with liposome-enriched nanofibers. The composite gel, however, is characterized not only by interesting drug uptake and release properties, but also by suitable biomechanical parameters for the construction of artificial cartilage. An optimal gel from the biomechanical point of view for osteochondral application still remains to be developed. Several gels prepared in various laboratories have been characterized by impact energy dissipation comparable to that of native cartilage (see e.g. Handl et al., 2010; Kerin et al., 1998). However, the mechanical stiffness and/or the Young's modulus of these materials has remained insufficient and in need of improvement. Our advanced nanofiber scaffold enriched with growth factors had a positive effect on cell recruitment and differentiation, and the addition of nanofibers also improved the mechanical properties of the composite gel. Adding nanofibers into the fibrin gel and also into the composite scaffold can improve the mechanical stiffness, and can in this way enhance the biomechanical properties almost to the parameters of the native articular cartilage. This effect can probably be explained by the effect of dispersed fiber reinforcement similar to that of the native material.

4.4. Growth factor-enriched cell-free PVA–liposome composite stimulated MSC recruitment from bone marrow in vivo

The in vitro findings on the growth factor release, cell culture, and biomechanics of the composite gel–nanofiber system were confirmed in our in vivo experiment. Functionalized nanofibers were cut into small pieces 1 × 2 mm in size. These particles served as a reservoir of continuously released growth factors, which subsequently diffused into the surrounding fibrin scaffold. Although the in vitro release rate for insulin was faster than for bFGF, 90% of the insulin was released within 9 days, and the absolute release was higher in liposome-containing nanofibers (PVA + LIP) than in pure PVA (Fig. 2). Our advanced nanofiber composite scaffold with attached liposomes enriched with growth factors was able

to enhance regeneration of the defect toward mostly fibrocartilage, while untreated defects were only partially filled with mostly dense irregular connective tissue. This advanced scaffold was shown to be a control drug delivery system preserving or prolonging the biological activity of the growth factors. The liposome-enriched nanofiber composite gel from hyaluronate/type I collagen/fibrin without cells suppressed the inflammatory reaction and the formation of osteophytes, and simultaneously stimulated the basis of the osteochondral defect into differentiation toward hyaline cartilage and/or fibrocartilage. The effect of the composite gel may have been positively influenced by hyaluronate, which had previously been reported to decrease hyluronate/fibrin gel degradation, and to enhance chondrocyte differentiation (Park et al., 2009). Hyaluronic acid had a more complex effect on cell behavior, probably also improving cell migration, proliferation and differentiation in addition to its effect on the viscoelastic properties of the scaffold. Moreover, type I collagen was able to improve the biomechanical properties of the composite scaffold (Filová et al., 2008).

Several techniques for stimulating bone marrow stem cell recruitment and/or migration into defects, e.g. microfracture and mosaicplasty, have been used in treating small chondral or osteochondral defects. However, predominantly dense irregular connective tissue or fibrocartilage were found to be formed. Unfortunately, the bone marrow stimulation techniques were less successful in patients over the age of 40 (Shapiro et al., 1993; Buckwalter and Lohmander, 1994). Cartilage regeneration can be improved by applying artificial scaffolds seeded either with chondrocytes or with mesenchymal stem cells (van Susante et al., 1999; Solchaga et al., 1999; Hunziker, 2001; Dorotka et al., 2005; Haleem et al., 2010). However, autologous chondrocyte and stem cells have shortcomings that hamper their use in clinical practice. Firstly, they need two surgeries that are demanding for patients. Secondly, the amount and also the quality of the available cells decreased with age (Leong and Sun, 2011), and, thirdly, cell cultivation requires a special cultivation system that raised the cost of the procedures. There are also problems associated with legal issues.

Cell-free approach based on platelet-rich fibrin glue has already been reported (Haleem et al., 2010; Kuo et al., 2011). However, the rapid degradation of growth factors in fibrin and also the insufficient biomechanical properties of fibrin limit the regenerative capacity of the scaffold.

In accordance with our observation, cell-free fibrin-containing TGF-β1 encapsulated in liposomes provided better cartilaginous tissue formation than TFG-β1 freely distributed in a fibrin gel (Hunziker, 2001). Growth factors encapsulated in liposomes or even bound to their surface are probably less susceptible to degradation. The composition and the biomechanical properties of the scaffold, and also the reservoir of growth factors enabling the controlled release of growth factors, are essential.

In conclusion, all this data supports the possible application of our composite scaffold containing nanofibers with liposomes functionalized with growth factors as a potential material for healing osteochondral defects. This advanced gel can be used for both cellular and acellular applications.

Acknowledgments

References

Alipour, S.M., Nouri, M., Mokhtari, J., Bahrami, S.H., 2009. Electrospinning of poly(vinyl alcohol)-water-soluble quaternized chitosan derivative blend. Carbohydr. Res. 344, 2496–2501.

Blundell, T.L., Cutfield, J.F., Dodson, G.G., Dodson, E., Hodgkin, D.C., Mercola, D., 1971. The structure and biology of insulin. Biochem. J. 125, 50P–51P.

Breinan, H.A., Minas, T., Hsu, H.P., Nehrer, S., Shortkroff, S., Spector, M., 2001. Autologous chondrocyte implantation in a canine model: change in composition of reparative tissue with time. J. Orthop. Res. 19, 482–492.

Brodwall, J., Alme, G., Gedde-Dahl, S., Smith, J., Lilliedahl, N.P., Kunz, P.A., Sunderraj, P.A., 1997. Comparative study of polyacrylic acid (Viscotears) liquid gel versus polyvinylalcohol in the treatment of dry eyes. Acta Ophthalmol. Scand. 75, 457–461.

Buckwalter, J.A., Lohmander, S., 1994. Operative treatment of osteoarthrosis. Current practice and future development. J. Bone Joint Surg. Am. 76, 1405–1418.

Buckwalter, J.A., Mankin, H.J., 1998. Articular cartilage: degeneration and osteoarthritis, repair, regeneration, and transplantation. Instr. Course Lect. 47, 487–504.

Buzgo, M., Jakubova, R., Mickova, A., Rampichova, M., Lukas, D., Amler, E. Time-regulated drug delivery system based on coaxially incorporated platelet alpha granules for biomedical use. Nanomedicine, in press.

Cherubino, P., Grassi, F.A., Bulgheroni, P., Ronga, M., 2003. Autologous chondrocyte implantation using a bilayer collagen membrane: a preliminary report. J. Orthop. Surg. (Hong Kong) 11, 10–15.

Dorotka, R., Bindreiter, U., Macfelda, K., Windberger, U., Nehrer, S., 2005. Marrow stimulation and chondrocyte transplantation using a collagen matrix for cartilage repair. Osteoarthritis Cartilage 13, 655–664.

Eshed, I., Trattnig, S., Sharon, M., Arbel, R., Nierenberg, G., Konen, E., Yayon, A., 2012. Assessment of cartilage repair after chondrocyte transplantation with a fibrin-hyaluronan matrix – correlation of morphological MRI, biochemical T2 mapping and clinical outcome. Eur. J. Radiol. 81, 1216–1223.

Filová, E., Rampichová, M., Handl, M., Lytvynets, A., Halouzka, R., Usvald, D., Hlucilová, J., Procházka, M., Dezortová, M., Rolencová, E., Kostáková, E., Trc, T., Stastný, E., Kolácná, L., Hájek, M., Motlík, J., Amler, E., 2007. Composite hyaluronate-type I collagen-fibrin scaffold in the therapy of osteochondral defects in miniature pigs. Physiol. Res. 56, S5–S16.

Filová, E., Jelínek, F., Handl, M., Lytvynets, A., Rampichová, M., Varga, F., Cinátl, J., Soukup, T., Trc, T., Amler, E., 2008. Novel composite hyaluronan/type I collagen/fibrin scaffold enhances repair of osteochondral defect in rabbit knee. J. Biomed. Mater. Res. B Appl. Biomater. 87, 415–424.

Firouznia, K., Ghanaati, H., Sanaati, M., Jalali, A.H., Shakiba, M., 2008. Uterine artery embolization in 101 cases of uterine fibroids: do size, location, and number of fibroids affect therapeutic success and complications? Cardiovasc. Intervent. Radiol. 31, 521–526.

Haleem, A.M., Singergy, A.A., Sabry, D., Atta, H.M., Rashed, L.A., Chu, C.R., El Shewy, M.T., Azzam, A., Abdel Aziz, M.T., 2010. The clinical use of human culture-expanded autologous bone marrow mesenchymal stem cells transplanted on platelet-rich fibrin glue in the treatment of articular cartilage defects: a pilot study and preliminary results. Cartilage 1, 253–261.

Handl, M., Držík, M., Varga, F., 2010. The current status of biomechanical evaluation of the hyaline cartilage. In: Brittberg, M., Imhoff, A., Madry, H., Mandelbaum, B. (Eds.), Cartilage Repair – Current Concepts. DJO Publications, London, pp. 23–31.

Holland, T.A., Mikos, A.G., 2003. Advances in drug delivery for articular cartilage. J. Control. Release 86, 1–14.

Hunziker, E.B., 2001. Growth-factor-induced healing of partial-thickness defects in adult articular cartilage. Osteoarthritis Cartilage 9, 22–32.

Hwang, M.R., Kim, J.O., Lee, J.H., Kim, Y.I., Kim, J.H., Chang, S.W., Jin, S.G., Kim, J.A., Lyoo, W.S., Han, S.S., Ku, S.K., Yong, C.S., Choi, H.G., 2010. Gentamicin-loaded wound dressing with polyvinyl alcohol/dextran hydrogel: gel characterization and in vivo healing evaluation. AAPS PharmSciTech. 11, 1092–1103.

Jakubova, R., Mickova, A., Buzgo, M., Rampichova, M., Prosecka, E., Tvrdik, D., Amler, E., 2011. Immobilization of thrombocytes on PCL nanofibres enhances chondrocyte proliferation in vitro. Cell Prolif. 44, 183–191.

Jannesari, M., Varshosaz, J., Morshed, M., Zamani, M., 2011. Composite poly(vinyl alcohol)/poly(vinyl acetate) electrospun nanofibrous mats as a novel wound dressing matrix for controlled release of drugs. Int. J. Nanomedicine 6, 993–1003.

Jelen, K., Lopot, F., Budka, Š., Nováček, V., Sedláček, R., 2008. Rheological properties of myometrium: experimental quantification and mathematical modeling. Neuro Endocrinol. Lett. 29, 454–460.

Jiang, T., Wang, G., Qiu, J., Luo, L., Zhang, G., 2009. Heparinized poly(vinyl alcohol) – small intestinal submucosa composite membrane for coronary covered stents. Biomed. Mater. 4, 025012.

Kang, S.W., Kim, J.S., Park, K.S., Cha, B.H., Shim, J.H., Kim, J.Y., Cho, D.W., Rhie, J.W., Lee, S.H., 2011. Surface modification with fibrin/hyaluronic acid hydrogel on solid-free form-based scaffolds followed by BMP-2 loading to enhance bone regeneration. Bone 48, 298–306.

Kerin, A.J., Wisnom, M.R., Adams, M.A., 1998. The compressive strength of articular cartilage. Proc. Inst. Mech. Eng. [H] 212, 273–280.

Konopasek, I., Kvasnicka, P., Amler, E., Kotyk, A., Curatola, G., 1995. The transmembrane gradient of the dielectric constant influences the DPH lifetime distribution. FEBS Lett. 374, 338–340.

Kuo, T.F., Lin, M.F., Lin, Y.H., Lin, Y.C., Su, R.J., Lin, H.W., Chan, W.P., 2011. Implantation of platelet-rich fibrin and cartilage granules facilitates cartilage repair in the injured rabbit knee: preliminary report. Clinics 66, 1835–1838.

Laurent, T.C., Fraser, J.R., 1992. Hyaluronan. FASEB J. 6, 2397–2404.

Leong, D.J., Sun, H.B., 2011. Events in articular chondrocytes with aging. Curr. Osteoporos. Rep. 9, 196–201.

Levchenko, T.S., Hartner, W.C., Torchilin, V.P., 2012. Liposomes for cardiovascular targeting. Ther. Deliv. 3, 501–514.

Litvinchuk, S., Lu, Z., Rigler, P., Hirt, T.D., Meier, W., 2009. Calcein release from polymeric vesicles in blood plasma and PVA hydrogel. Pharm. Res. 26, 1711–1717.

Liu, X., Lin, T., Fang, J., Yao, G., Zhao, H., Dodson, M., Wang, X., 2010. In vivo wound healing and antibacterial performances of electrospun nanofibre membranes. J. Biomed. Mater. Res. A 94, 499–508.

Longo, U.G., Campi, S., Romeo, G., Spiezia, F., Maffulli, N., Denaro, V., 2012. Biological strategies to enhance healing of the avascular area of the meniscus. Stem Cells Int. 2012, 528924.

Lukáš, D., Sarkar, A., Pokorný, P., 2008. Self organization of jets in electrospinning from free liquid surface – a generalized approach, accepted for publication. J. Appl. Phys. 103, 309–316.

Luong-Van, E., Grøndahl, L., Chua, K.N., Leong, K.W., Nurcombe, V., Cool, S.M., 2006. Controlled release of heparin from poly(epsilon-caprolactone) electrospun fibers. Biomaterials 27, 2042–2050.

Maniwa, S., Ochi, M., Motomura, T., Nishikori, T., Chen, J., Naora, H., 2001. Effects of hyaluronic acid and basic fibroblast growth factor on motility of chondrocytes and synovial cells in culture. Acta Orthop. Scand. 72, 299–303.

Marlovits, S., Striessnig, G., Kutscha-Lissberg, F., Resinger, C., Aldrian, S.M., Vecsei, V., Trattnig, S., 2005. Early postoperative adherence of matrix-induced autologous chondrocyte implantation for the treatment of full-thickness cartilage defects of the femoral condyle. Knee Surg. Sports Traumatol. Arthrosc. 13, 451–457.

McCarron, P.A., Murphy, D.J., Little, C., McDonald, J., Kelly, O.J., Jenkins, M.G., 2011. Preliminary clinical assessment of polyvinyl alcohol-tetrahydroxyborate hydrogels as potential topical formulations for local anesthesia of lacerations. Acad. Emerg. Med. 18, 333–339.

Mickova, A., Buzgo, M., Benada, O., Rampichova, M., Fisar, Z., Filova, E., Tesarova, M., Lukas, D., Amler, E., 2012. Core/shell nanofibers with embedded liposomes as a drug delivery system. Biomacromolecules 13, 952–962.

Park, J.S., Shim, M.S., Shim, S.H., Yang, H.N., Jeon, S.Y., Woo, D.G., Lee, D.R., Yoon, T.K., Park, K.H., 2011a. Chondrogenic potential of stem cells derived from amniotic fluid, adipose tissue, or bone marrow encapsulated in fibrin gels containing TGF-b3. Biomaterials 32, 8139–8149.

Park, S.H., Cui, J.H., Park, S.R., Min, B.H., 2009. Potential of fortified fibrin/hyaluronic acid composite gel as a cell delivery vehicle for chondrocytes. Artif. Organs 33, 439–447.

Park, S.J., Choi, S.G., Davaa, E., Park, J.S., 2011b. Encapsulation enhancement and stabilization of insulin in cationic liposomes. Int. J. Pharm. 415, 267–272.

Pham, Q.P., Sharma, U., Mikos, A.G., 2006. Electrospun poly(epsilon-caprolactone) microfiber and multilayer nanofiber/microfiber scaffolds: characterization of scaffolds and measurement of cellular infiltration. Biomacromolecules 7, 2796–2805.

Pittenger, M.F., Mackay, A.M., Beck, S.C., Jaiswal, R.K., Douglas, R., Mosca, J.D., Moorman, M.A., Simonetti, D.W., Craig, S., Marshak, D.R., 1999. Multilineage potential of adult human mesenchymal stem cells. Science 1999, 143–147.

Prosecká, E., Buzgo, M., Rampichová, M., Kocourek, T., Kochová, P., Vysloužilová, L., Tvrdík, D., Jelínek, M., Lukáš, D., Amler, E., 2012. Thin-layer hydroxyapatite deposition on a nanofiber surface stimulates mesenchymal stem cell proliferation and their differentiation into osteoblasts. J. Biomed. Biotechnol. 2012, 1–10, Article ID 428503.

Radice, M., Brun, P., Cortivo, R., Scapinelli, R., Battaliard, C., Abatangelo, G., 2000. Hyaluronan-based biopolymers as delivery vehicles for bone-marrow-derived mesenchymal progenitors. J. Biomed. Mater. Res. 50, 101–109.

Rampichová, M., Martinová, L., Košťáková, E., Filová, E., Míčková, A., Buzgo, M., Michálek, J., Přádný, M., Nečas, A., Lukáš, D., Amler, E., 2012. A simple drug anchoring microfiber scaffold for chondrocyte seeding and proliferation. J. Mater. Sci. Mater. Med. 23, 555–563.

Sahoo, S., Ang, L.T., Goh, J.C.H., Toh, S.L., 2010a. Growth factor delivery through electrospun nanofibres in scaffolds for tissue engineering applications. J. Biomed. Mater. Res. A 93, 1539–1550.

Sahoo, S., Ang, L.T., Goh, J.C.H., Toh, S.L., 2010b. Bioactive nanofibers for fibroblastic differentiation of mesenchymal precursor cells for ligament/tendon tissue engineering applications. Differentiation 79, 102–110.

Schwinke, D.L., Ganesan, M.G., Weiner, N.D., 1983. Monolayer studies of insulin-lipid interactions. J. Pharm. Sci. 72, 244–248.

Senna, M.M., Salmieri, S., El-Naggar, A.W., Safrany, A., Lacroix, M., 2010. Improving the compatibility of zein/poly(vinyl alcohol) blends by gamma irradiation and graft copolymerization of acrylic acid. J. Agric. Food Chem. 14, 4470–4476.

Shapiro, F., Koide, S., Glimcher, M.J., 1993. Cell origin and differentiation in the repair of full-thickness defects of articular cartilage. J. Bone Joint. Surg. Am. 75, 532–553.

Spicer, P.P., Mikos, A.G., 2010. Fibrin glue as a drug delivery system. J. Control. Release 20, 49–55.

Solchaga, L.A., Dennis, J.E., Goldberg, V.M., Caplan, A.I., 1999. Hyaluronic acid-based polymers as cell carriers for tissue-engineered repair of bone and cartilage. J. Orthop. Res. 17, 205–213.

Sun, H.H., Qu, T.J., Zhang, X.H., Yu, Q., Chen, F.M., 2012. Designing biomaterials for in situ periodontal tissue regeneration. Biotechnol. Prog. 28, 3–20.

Trattnig, S., Ba-Ssalamah, A., Pinker, K., Plank, C., Vecsei, V., Marlovits, S., 2005. Matrix-based autologous chondrocyte implantation for cartilage repair: non-invasive monitoring by high-resolution magnetic resonance imaging. Magn. Reson. Imaging 23, 779–787.

Ulrich, A.S., 2002. Biophysical aspects of using liposomes as delivery vehicles. Biosci. Rep. 22, 129–150.

van Susante, J.L., Buma, P., Schuman, L., Homminga, G.N., van den Berg, W.B., Veth, R.P., 1999. Resurfacing potential of heterologous chondrocytes suspended in fibrin glue in large full-thickness defects of femoral articular cartilage: an experimental study in the goat. Biomaterials 20, 1167–1175.

Vaquero, J., Forriol, F., 2012. Knee chondral injuries: clinical treatment strategies and experimental models. Injury 43, 694–705.

Varga, F., Drzík, M., Handl, M., Chlpík, J., Kos, P., Filová, E., Rampichová, M., Necas, A., Trc, T., Amler, E., 2007. Biomechanical characterization of cartilages by a novel approach of blunt impact testing. Physiol. Res. 56, S61–S68.

Visna, P., Pasa, L., Cizmár, I., Hart, R., Hoch, J., 2004. Treatment of deep cartilage defects of the knee using autologous chondrograft transplantation and by abrasive techniques – a randomized controlled study. Acta Chir. Belg. 104, 709–714.

Walker, J., Young, G., Hunt, C., Henderson, T., 2007. Multi-centre evaluation of two daily disposable contact lenses. Cont. Lens Anterior Eye 30, 125–133.

Wiessner, J.H., Hwang, K.J., 1982. Binding of insulin to the external surface of liposomes. Effect of surface curvature, temperature, and lipid composition. Biochim. Biophys. Acta 689, 490–498.